Integrated Separation Columns and Fabry-Perot Sensors for Microgas Chromatography Systems

Karthik Reddy, Jing Liu, Maung Kyaw Khaing Oo, and Xudong Fan

***Abstract*—We developed a monolithic subsystem that integrates a microgas chromatography (μGC) separation column and on-column, nondestructive Fabry-Pérot (FP) vapor sensors on a single silicon chip. The device was fabricated using deep reactive ion etching of silicon to create fluidic channels and polymers were deposited on the same silicon chip to act as a stationary phase or an FP sensor, thus avoiding dead volumes caused by the interconnects between the column and sensor traditionally used in μGC. Two integration designs were studied. In the first design, a 25-cm long μGC column was coated with a layer of polymer that served as both the stationary phase and the FP sensor, which has the greatest level of integration. This design was capable of sub-second response times and detection limits under 10 ng. In the second design, an FP sensor array spray coated with different vapor sensing polymers was integrated with a 30-cm long μGC column, which significantly improves the system flexibility and detection sensitivity. With this design, we show that the FP sensors have a detection limit on the order of tens of picograms or ∼500 ppb with a sub-second response time. Furthermore, the FP sensor array are shown to respond to a mixture of analytes separated by the integrated separation channel, allowing for the construction of response patterns, which, along with retention time, can be used as a basis of analyte identification. [2012-0305]**

***Index Terms*—Vapor sensing, optical vapor sensor, Fabry-Pérot cavity, microgas chromatography, MEMS, separation columns.**

I. Introduction

THE increasing need for on-site volatile organic compound (VOC) detection has led to intense development of microgas chromatography (μGC) systems [1]–[4]. A typical μGC system utilizes several silicon or MEMs-based components, including preconcentrators [5]–[7], separation columns [8]–[13], and detectors [14]–[23]. Traditionally, each of those components is fabricated separately and then connected together. While fabrication of stand-alone components is relatively straightforward, the subsequent assembly is mainly accomplished manually, which is time-consuming, prone to errors, and incompatible with future mass production. In addition, the system such made is not only large in footprint, but also has a dead volume resulting from interconnects [24]–[26], which may adversely affect the μGC performance. Therefore, a monolithic subsystem that integrates multiple components on a single-chip is highly desirable.

As the first step toward a completely integrated μGC system, here we aim to incorporate the separation columns with vapor sensing elements. In particular, we are interested in developing an on-column nondestructive vapor sensor (or sensors) that can detect VOCs traveling through the microfluidic channel without interruption to or interference with the flow, thus providing unique capability for novel μGC designs [27]. On-column nondestructive vapor sensors have previously been demonstrated using thermal conductivity detectors (TCDs) [28]. In particular, progress has recently been made toward integrating the TCD with the separation columns [29]–[31]. On-column nondestructive vapor sensing has also been carried out with optical sensors, such as capillary-based optical ring resonators [20], [32]–[34], Fabry-Pérot (FP) sensors fabricated on an optical fiber facet [27], [35]–[37], and stand-alone FP sensors fabricated on a silicon chip [19], [38], which have very small footprint (μm), an excellent detection limit (∼1 pg), and ability to perform arrayed detection.

In this paper, we introduce two designs that integrate the μGC separation column with on-chip FP sensors. In the first design illustrated in Fig. 1(A), the microfabricated column is coated with a layer of polymer that serves as both the stationary phase and the FP sensor. The advantages of this design include 1) significantly simplified integration of the column and vapor sensor, (2) elimination of the dead volume arising from the column/sensor connection, and (3) built-in vapor sensor along the column (detection can be carried out at any location and multiple detection positions can also be implemented so that the separation process can be monitored in real time [20]). On the other hand, this design has several drawbacks because it lacks flexibility in selecting polymers (as the polymer is the same as that for the stationary

Manuscript received October 22, 2012; revised March 17, 2013; accepted March 18, 2013. Date of publication June 20, 2013; date of current version September 27, 2013. This work was supported in part by the National Science Foundation (IOS 0946735) and in part by the Lurie Nanofabrication Facility at the University of Michigan. Subject Editor C. H. Mastrangelo.

K. C. Reddy is with the Department of Biomedical Engineering, Department of Electrical Engineering and Computer Science, Center for Wireless Integrated Microsensing and Systems, University of Michigan, Ann Arbor, MI 48109 USA (e-mail: karreddy@umich.edu).

J. Liu is with the Department of Biomedical Engineering, Center for Wireless Integrated Microsensing and Systems, University of Michigan, Ann Arbor, MI 48109 USA.

M. K. K. Oo and X. Fan are with the Department of Biomedical Engineering, University of Michigan, Ann Arbor, MI 48109 USA.

This paper has supplementary downloadable material available at http://ieeexplore.ieee.org provided by the authors. The material consists of one PDF file containing seven figures and corresponding captions. The size of the file is 317 KB. contact: xsfan@umich.edu for further questions about this work.

Color versions of one or more of the figures in this paper are available online at http://ieeexplore.ieee.org.

Digital Object Identifier 10.1109/JMEMS.2013.2262582

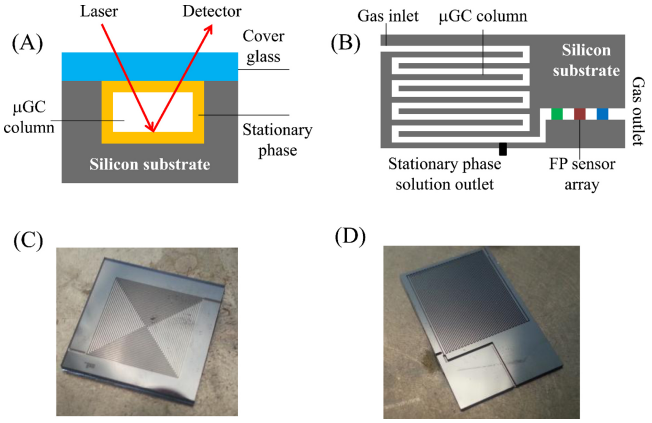

Fig. 1. Cross-sectional view of first design to integrate the μGC column with on-column vapor sensor, in which polymer coating is used as both stationary phase and on-column FP vapor sensor. Detection can be carried out at any location along the column. (B) Top view of the second design to integrate the μGC column with the on-column FP vapor sensor array. Different polymer coating can be used for column and FP sensors. (C) Image of a 25-cm long μGC separation column fabricated on silicon based on the first design illustrated in (A). Column depth = 150 μm and width = 240 μm. (D) Image of fabricated integrated μGC separation column and the FP sensors based on the second design illustrated in (B). Column length = 30 cm, depth = 400 μm, and width = 120 μm.

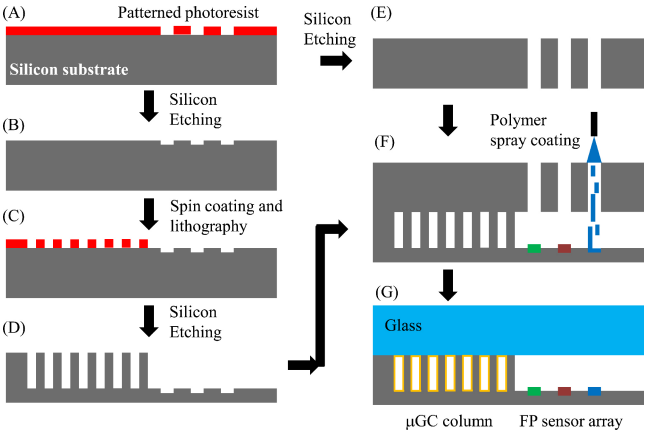

Fig. 2. Fabrication process of the device for the second design. (A) Photoresist was spun onto silicon and patterned using UV photolithography. (B) 1-μm Deep reactive ion etching (DRIE) of silicon to define the sensor area. (C) Photoresist was spun on the etched wafer and patterned with UV lithography. (D) Column was etched using DRIE. (E) Shadow mask fabricated by DRIE through etching of another silicon wafer. (F) Spray coating of the sensor polymers at desired locations with aid of the shadow mask. (G) Glass top wafer was bonded to the silicon wafer and the column was coated with polymer as a stationary phase. The detail of the stationary phase coating process are illustrated in Fig. S1. (available at http://ieeexplore.ieee.org).

phase) and it may be difficult to simultaneously optimize the polymer coating for both separation and sensing. Usually the polymer and its coating processes are optimized for best separation. As a result, the sensing performance may be compromised.

Another design illustrated in Fig. 1(B) overcomes the aforementioned issues. The separation column and sensors are fabricated on the same monolithic chip. Meanwhile, different polymers and coating processes are used so that both stationary phase and FP sensor are optimized for best separation and sensing, respectively. In addition, multiple FP sensors can be built with different polymers to generate response patterns for better identification of VOCs [19].

II. Materials, Fabrication and Methods

A. Materials

Silicon and Pyrex wafers were purchased from University Wafer (South Boston, MA). UV-curable optical glues were purchased from Dymax (Torrington, CT) and Norland (Cranbury, NJ). OV-1 (poly(dimethylsiloxane) or PDMS), OV-215 (trifluoropropylmethylsilicone), and OV-1701 (dimethylphenyl cyano substituted) were purchased from Ohio Valley Specialty (Marietta, OH). GC guard column (part no. 10029, inner diameter 250 μm) was purchased from Restek (Bellefonte, PA) and universal quick seal column connectors were purchased from Varian (Palo Alto, CA). All analytes and solvents used in the experiments were purchased from Sigma (St. Louis, MO) and had purity greater than 97%. All materials were used as received.

B. Fabrication

OV-1 and OV-215 were chosen for use as the stationary phase and OV-1, OV215, or OV-1701 was used as the vapor sensing polymer coating. The polymer solutions were prepared by dissolving the polymer gum in their corresponding solvent. For use in separation column stationary phase, OV-1 was diluted with a mixture of 1:1 (v:v) pentane and dichloromethane (OV-1:pentane/dichloromethane = 10 mg:3 ml), whereas OV-215 solution was prepared by dissolving 20 mg OV-215 and 0.2 mg dicumyl peroxide in a 5 ml mixture of 1:4 (v:v) ether and ether acetate. For the purpose of the sensors OV-1 was diluted with toluene (PDMS:toluene = 10 mg:1 ml), OV-1701 was diluted with pentane (OV-1701:pentane = 10 mg:1 ml), and OV-215 was diluted with ethyl acetate (OV-215:ethyl acetate = 10 mg:1 ml).

For the first design, the μGC column was fabricated using an MA-6 and STS Pegasus-4 for lithography and deep reactive ion etching of a 25-cm channel, with a footprint of only 1.1 cm^2. Then a Pyrex cover sheet was anodically bonded to the silicon substrate to seal the channel. The rectangular cross section of the channel was 150 μm by 240 μm. Finally, the channel was coated with the desired polymer by (OV-1 or OV-215) 1) filling the column with the previously prepared coating solution and holding for 5 min; 2) evaporating the solution from one end of the column using a vacuum pump while the sealing the other end with a septum; 3) cross-linking the polymer to the inner wall of the column by ramping the column temperature from 160 to 180 degC at a rate of 0.2 degC/min and staying at 180 degC for 1 h. The resultant column coating had a uniform thickness of around 200 nm. The fabricated column is shown in Fig. 1(C) [39].

The complete fabrication procedure for the second design (i.e., the integrated separation column and FP sensor array) is illustrated in Figs. 2 and S1 (available at http://ieeexplore.ieee.org). First, three 1.2-μm deep wells were etched into the prime grade silicon. These wells were designed to act as containment for polymers as well as visual markers for subsequent optical vapor detection (Section II-C).

Each well was 200 μm $\times$ 200 μm and were separated by 800 μm. Next, the silicon was patterned and etched to form the serpentine separation column. Close attention was paid to alignment so that the etched wells were within the column. The column was approximately 400-μm deep and 120-μm wide. The higher aspect ratio of these columns compared to the first design allows for better performance at higher flow rates. There is no change in sensitivity of the polymers to analytes arising from the change in column dimensions. Then, a shadow mask was fabricated by through-etching a silicon wafer such that the holes aligned with the containment wells on the first silicon wafer. After alignment, we created an FP sensor array by spray coating the aforementioned polymer solutions, using an Iwada HP-B + airbrush, onto the pre-etched wells. The polymer thickness can be controlled by the coating time and polymer solution concentration. For the present paper, all polymer coatings were approximately 1-μm thick [measured using the free spectral range of the interference pattern obtained using a white light source and spectrometer, Fig. S2 (available at http://ieeexplore.ieee.org)]. By using the shadow mask and spray coating, cross contamination of polymers between the adjacent wells is eliminated. In the final step, a diced Pyrex wafer was bonded to the silicon wafer using UV-curable optical glue prior to static coating of the column with OV-1. The optical glue was carefully applied to the devices to minimize contamination of the channels. Also, once cured the optical glue is very inert and should have no effect on the analytes. The bond can tolerate up to at least 10 psi flow pressure which is sufficient for μGC applications. The optical glue used has a thermal limit of 190 degC, which imposes an upper limit on the maximum operating temperature of this system.

To prevent any overflow of the stationary phase solution onto the sensor array we designed a stationary phase solution outlet near the end of the separation column [see Fig. 1(B)], through which the polymer solution was withdrawn from the gas inlet side while sealing the distal end of the device (i.e., gas outlet near the FP sensor array). The detail of the stationary phase coating process is described in Fig. S1 (available at http://ieeexplore.ieee.org). The completed device is shown in Fig. 1(D). The dead volume due to the presence of the stationary phase solution outlet, which was sealed after the coating process was complete, is estimated to be less than 1 nl, much smaller than microliter dead volumes reported previously [24]–[26].

The fabrication procedure which involves depositing polymer prior to bonding the silicon and glass substrates precludes the use of anodic bonding due to the high temperatures involved in the process. However, using an optical epoxy to bond the substrates lowers the yield and throughput substantially compared to regular μGC column fabrication. Issues arise from improper bonding and gaps in the substrate which necessitates extreme care during application of the adhesive. Additionally, we studied the potential outgassing effects of the adhesive the column during temperature ramping. In this case, a standard GC guard column, an anodically bonded μGC column coated with PDMS, and an uncoated μGC column bonded using an optical adhesive were tested with an FID. According to Fig. S3 (available at http://ieeexplore.ieee.org), the guard column shows a small change in the chromatographic response under temperature ramping, about 2 mV, the effect of the anodically bonded PDMS coated μGC column is about six times greater than the guard column, about 11 mV, and the uncoated optical adhesive bonded column has a response about five times larger than the anodically bonded column, about 55 mV. The above results indicate that there is indeed an outgassing effect due to the adhesive which will eventually affect the detection limit of the sensors. However, the slow increase in the baseline and subsequent plateau that the baseline reaches when the temperature stabilizes does not resemble the sharp peaks the analytes produce.

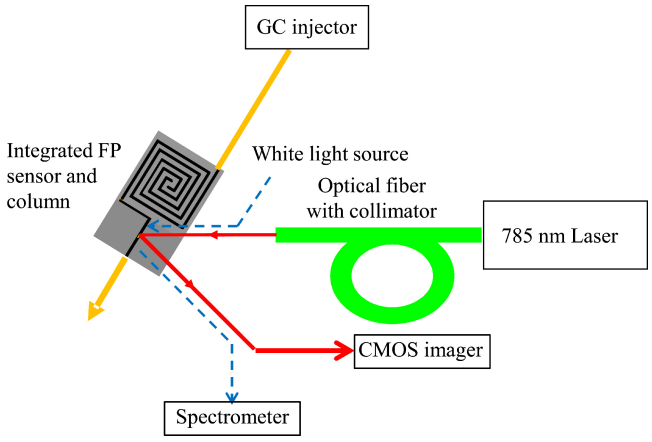

Fig. 3. Schematic of the fluidic and optical detection setup. A 785-nm laser was used to illuminate the entire FP sensor array. White light colinear with the laser beam was used to adjust the incident angle to maximize sensitivity. The CMOS imager was used to simultaneously monitor the change in reflected intensity in all three FP sensors caused by the interaction between the vapor analyte with the FP sensors.

C. Experimental Setup

The experimental setup is illustrated in Fig. 3. Analytes were injected at the GC injection port and delivered to the FP sensors or sensors array through a 4-m long GC guard column. To illuminate the FP sensors a Toptica 785 nm laser was aligned using an FC/APC terminated optical fiber and a beam collimator. The principle of the FP vapor sensor is described in Fig. S4 (available at http://ieeexplore.ieee.org). The reflected beam was collected by a Thorlabs CMOS imager (product no. DCC1545 M), attached to a lens (VZM450; Edmund Optics) to capture all FP sensors simultaneously. The reference signal was also acquired from the laser light reflected from the bare silicon surface and used to remove any long-term laser intensity drifts or false peaks caused by laser instability. The acquisition rate on the imager was set at 20 fps for all tests. To maximize the sensors' sensitivity by tuning the beam incident angle, a white light source was placed colinearly with the laser beam and at the reflection side a spectrometer (Ocean Optics HR-2000) was used to monitor the interference spectrum (dashed lines in Fig. 3). The flow rate for testing individual analytes was set at 8 mL/min.

To test the separation capability of the columns, a liquid mixture containing multiple analytes was injected at the GC injection port. It was delivered to the microfabricated GC

column to separate the mixture before detection by the FP sensor. The overall optical detection setup remained the same, as previously described. To enhance separation of analytes, the flow rate was done a multiple flow rates ranging from 1 to 4 ml/min. All experiments were carried out at room temperature with no heating of the columns or sensors. Mass of injected analytes was calibrated using a splitter and mass spectroscopy system. Helium was used as the carrier gas in all experiments.

III. Results and Discussion

First, we tested the separation and sensing capability of the first design [Fig. 1(A)], where the stationary phase was also used as the vapor sensing polymer. Fig. 4(A) and (C) and Fig. S5 (available at http://ieeexplore.ieee.org) show the chromatograms obtained by injecting a mixture of three analytes (toluene, octane, and decane). The response rose rapidly in the presence of analyte and rapidly fell back to the baseline as the analyte was purged. The above result suggests that the polymer coating inside a μGC column indeed can be used for dual purposes (i.e., stationary phase and sensing). Since the CMOS imager was operated at 20 fps, a system time resolution of 50 ms can be achieved. The sensitivity curves of the OV-1 and OV-215 stationary phase FP sensor are plotted in Fig. 4(B) and (D), respectively, revealing the dependence of the peak height on the injected analyte mass. To estimate the detection limit, we used the lowest data point in Fig. 4(B) in combination with the sensor noise level of approximately 0.1 counts. Decane exhibited the best detection limits of 2.6 and 6.1 ng for the OV-1 and OV-215 sensors, respectively, while octane and toluene had a detection limit of 4.6 and 10 ng, with OV-1 and 11.5 and 9.4 ng with OV-215. The principle of this design is valid regardless of polymer or its thickness.

While the design demonstrated above is superior in its level of integration and detection simplicity, the sensitivity is inferior to the optical vapor sensors that we have developed [19]. This low sensitivity can be attributed to thickness of the polymer (~200 nm), which is far thinner than previously demonstrated FP sensors, and the insufficient polymer coating uniformity when compared to spin or spray-coated polymer layers, and, therefore, poses a challenge for this design to be considered in a viable μGC system without further significant improvement in the sensitivity.

In the second design [Fig. 1(B)], by separating the sensing element and separation column while keeping them on the same chip we can overcome the aforementioned issues and develop an integrated separation and sensing system. To characterize the device's sensitivity, we placed the FP sensor array right after the 4-m long guard column by inserting it to the gas outlet on the chip [see Fig. 1(B)], thus bypass the μGC column. Each FP sensor was tested with three different analytes (acetone, toluene, and octane). The peak response of each sensor and analyte is shown in Fig. 5. The response is linear at lower injected mass and tends to saturate as the injected mass is increased. At the higher masses there is also peak broadening, which appears to indicate sensor overloading.

The interaction of analytes with polymers is affected by various factors including their polarities, functional groups,

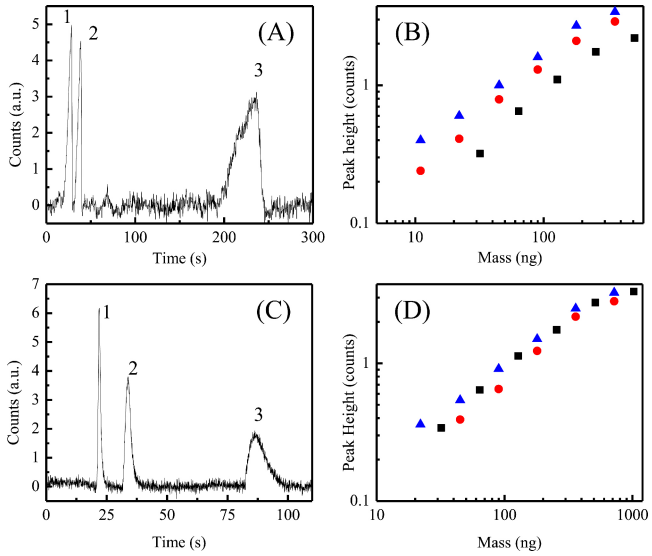

Fig. 4. Chromatographic response of the OV-1 polymer coating inside a μGC column to a mixture of toluene (1.6 μg, #1), octane (1.4 μg, #2), and decane (2 μg, #3) at 2 ml/min. (B) Response of the OV-1 polymer coating inside a μGC column to toluene (squares), octane (circles), and decane (triangles). (C) Chromatographic response of the OV-215 polymer coating inside a μGC column to a mixture of octane (2 μg, #1), toluene (1.6 μg, #2), and decane (1.8 μg, #3) at 2 ml/min. (D) Response of the OV-215 polymer coating inside a μGC column to toluene (squares), octane (circles), and decane (triangles). Additional chromatographic responses are shown in Fig. S4. (available at http://ieeexplore.ieee.org)

molecular weight, and volatility, and so on. By using three different polymers with varying polarities it is possible to build a sensor array. Using a sensor array can be a valuable aid in analyte identification. Additionally, the sensor array can comprise polymers that are different from the polymer stationary phase, thereby increasing the flexibility of the system. From the sensitivity curves shown in Figs. 5 and S6 (available at http://ieeexplore.ieee.org), it is clear that the different polymers have different sensitivities and different detection limits, depending on their interaction with each analyte. The best detection limit, calculated by using the lowest data point and a noise level of 0.1 counts, was found to be 40 pg for OV-1 and octane. While OV-1 also had the best detection limit for toluene at 44 pg, the best detection limit for acetone was exhibited by OV-215 at 80 pg. Based on the retention time (4–5 s) and the peak width (~0.25–0.4 s), as well as the inner diameter (250 μm) and length (4 m) of the GC guard column, the above detection limits, in concentration at atmospheric pressure, corresponds to about 504 ppb for octane, 700 ppb for toluene, and 900 ppb for acetone. While the detection limits of these sensors are not as low as those demonstrated by us previously (~30 ppb) [19], [40], they are similar to the reported results for micro-TCD [28] and carbon-nanotube FETs [22], and better than those for chemiresistors [14], SAW sensors [18], and microplasma detectors [21], as well as the nanoresonator sensors developed recently that has a sub-ppb or attogram detection limit in theory, but only 1 ng detection limit in practical GC applications [23]. It is important to note that while different FP sensors may have slightly different noise levels, because of surface roughness of the polymer and scattering of the optical beam, these differences are very small and

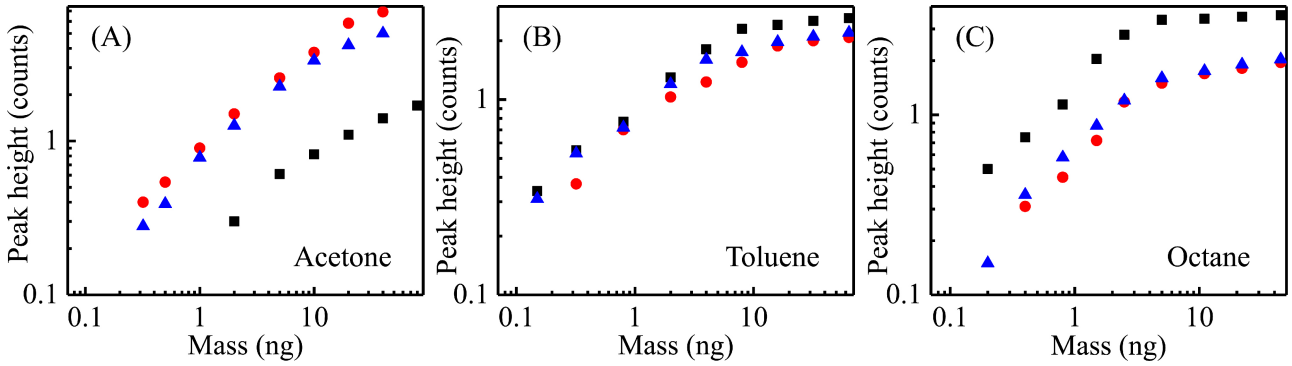

Fig. 5. Response of three different polymers OV-1 (squares), OV-215 (circles), and OV-1701 (triangles) to various injected masses of (A) acetone, (B) toluene, and (C) octane. The linear–linear plots are presented in Fig. S5 (available at http://ieeexplore.ieee.org).

are not a major factor in the different detection limits of each sensor.

To demonstrate the separation capability of the column along with the rapid simultaneous detection of eluted analytes by the sensor array. Figs. 6(A) and S7 (available at http://ieeexplore.ieee.org) show the chromatograms obtained from each polymer for a mixture of five analytes separated, at different flow rates, by the integrated column/sensor system [Fig. 1(B) and (D)]. Due to the high-linear speed of the analyte traveling inside the microfluidic channel, all FP sensors in the array were able to detect the same analyte virtually simultaneously. The peak height is used to extract response patterns for each analyte. Fig. 6(B)–(F) illustrate the response patterns for the injected mixture shown in Fig. 6(A). The response patterns clearly differ for each injected analyte, and concur with the previous testing results shown in Fig. 5. The error bars show a variation of less than 16% among runs, which will not limit the use of response patterns as a method of analyte identification in conjunction with the analyte retention time.

IV. Conclusion and Future Work

We have fabricated and characterized two subsystem designs that integrates the μGC column and FP sensor (array), which are robust, reproducible, and fast in response, and can potentially improve the efficiency and reduce the size of μGC systems. In particular, the second design where a sensor array was used demonstrated the ability to separate multiple analytes and simultaneously gather information from multiple sensors to conduct pattern analysis for qualitative and quantitative detection of VOC mixtures. The detection limit for the sensor is on the order of tens of picograms. Future work will focus on fabrication procedures, particularly polymer coating and low temperature substrate bonding, such as eutectic bonding [41], to improve the yield and sensitivity. In addition, a subsystem with a higher level of integration will be developed, which will include on-chip preconcentrators [6], [42], [43] and on-chip thermal modulators or injector [44], as well as temperature ramping.[1]

[1]Note: the polymers used by the FP sensors are routinely used in GC columns as the stationary coating. Therefore, no polymer degradation is expected to arise from temperature ramping.

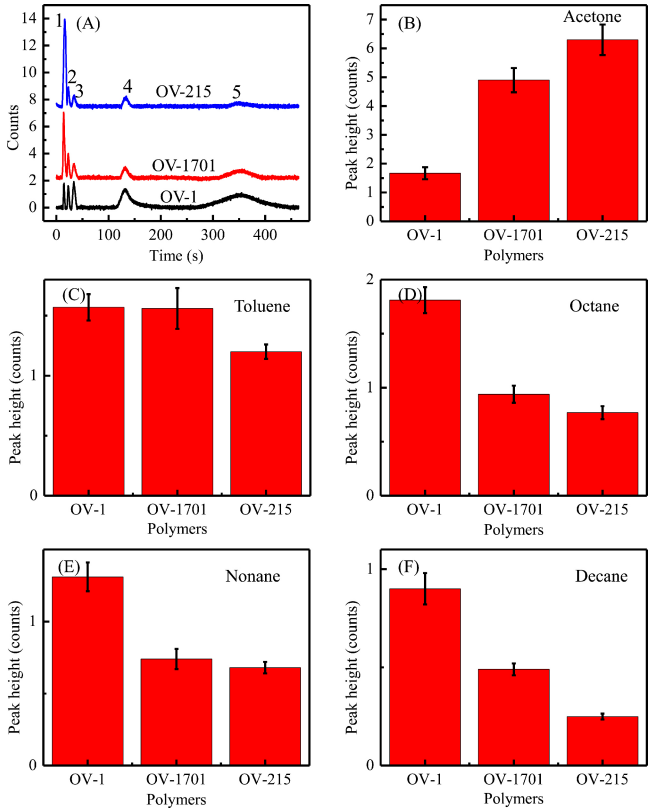

Fig. 6. Chromatographic response of three polymers on-chip to a mixture of acetone (60 ng, #1), toluene (45 ng, #2), octane (25 ng, #3), nonane (45 ng, #4), and decane (50 ng, #5) at 2 ml/min. (B)–(F) Response patterns of each analyte with respect to the three polymers on-chip for chromatogram shown in (A). Error bars show the standard deviation of 5 runs.

References

[1] F. L. Dorman, J. J. Whiting, J. W. Cochran, and J. Gardea-Torresdey, "Gas Chromatography," *Anal. Chem.*, vol. 82, no. 12, pp. 4775–4785, 2010.

[2] E. J. Staples, T. Matsuda, and S. Viswanathan, "Real time environmental screening of air, water and soil matrices using a novel field portable GC/SAW system," presented at the Environ. Strat. 21st Cent. Asia Pacific Conf., Singapore, 1998.

[3] K. Hanseup, W. H. Steinecker, S. Reidy, G. R. Lambertus, A. A. Astle, K. Najafi, E. T. Zellers, L. P. Bernal, P. D. Washabaugh, and K. D. Wise, "A micropump-driven high-speed MEMS gas chromatography system," in *Proc. Solid-State Sens. Act. Microsys. Conf.*, Lyon, France, 2007, pp. 1505–1508.

[4] R. Manginell, J. Bauer, M. Moorman, L. Sanchez, J. Anderson, J. Whiting, D. Porter, D. Copic, and K. Achyuthan, "A monolithically-integrated μGC chemical sensor system," *Sensors*, vol. 11, no. 7, pp. 6517–6532, 2011.

[5] B. Alfeeli and M. Agah, "MEMS-based selective preconcentration of trace level breath analytes," *IEEE Sens. J.*, vol. 9, no. 9, pp. 1068–1075, Sep. 2009.

[6] J. H. Seo, S. K. Kim, E. T. Zellers, and K. Kurabayashi, "Microfabricated passive vapor preconcentrator/injector designed for microscale gas chromatography," *Lab Chip*, vol. 12, no. 4, pp. 717–724, 2012.

[7] T. Sukaew, H. Chang, G. Serrano, and E. T. Zellers, "Multi-stage preconcentrator/focuser module designed to enable trace level determinations of trichloroethylene in indoor air with a microfabricated gas chromatograph," *Analyst*, vol. 136, no. 8, pp. 1664–1674, 2011.

[8] G. Lambertus, A. Elstro, K. Sensenig, J. Potkay, M. Agah, S. Scheuering, K. Wise, F. Dorman, and R. Sacks, "Design, fabrication, and evaluation of microfabricated columns for gas chromatography," *Anal. Chem.*, vol. 76, no. 9, pp. 2629–2637, 2004.

[9] M. Agah, J. A. Potkay, G. Lambertus, R. Sacks, and K. D. Wise, "High-performance temperature-programmed microfabricated gas chromatography columns," *J. Microelectromech. Syst.*, vol. 14, no. 9, pp. 1039–1050, 2005.

[10] N. Hong-seok, P. J. Hesketh, and G. C. Frye-Mason, "Parylene gas chromatographic column for rapid thermal cycling," *J. Microelectromech. Syst.*, vol. 11, no. 5, pp. 718–725, 2002.

[11] M. A. Zareian-Jahromi, M. Ashraf-Khorassani, L. T. Taylor, and M. Agah, "Design, modeling, and fabrication of MEMS-based multicapillary gas chromatographic columns," *J. Microelectromech. Syst.*, vol. 18, no. 6, pp. 28–37, 2009.

[12] J. A. Potkay, G. R. Lambertus, R. D. Sacks, and K. D. Wise, "A low-power pressure- and temperature-programmable micro gas chromatography column," *J. Microelectromech. Syst.*, vol. 16, no. 1, pp. 1071–1079, 2007.

[13] J. A. Potkay, J. A. Driscoll, M. Agah, R. D. Sacks, and K. D. Wise, "A high-performance microfabricated gas chromatography column," in *Proc. Int. Conf. Microelectromech. Syst.*, Kyoto, Japan, 2003, pp. 395–398.

[14] Q.-Y. Cai and E. T. Zellers, "Dual-chemiresistor GC detector employing monolayer-protected metal nanocluster interfaces," *Anal. Chem.*, vol. 74, no. 14, pp. 3533–3539, 2002.

[15] C. K. Ho and R. C. Hughes, "In-situ chemiresistor sensor package for real-time detection of volatile organic compounds in soil and groundwater," *Sensors*, vol. 2, no. 1, pp. 23–34, 2002.

[16] E. Covington, F. I. Bohrer, C. Xu, E. T. Zellers, and C. Kurdak, "Densely integrated array of chemiresistor vapor sensors with electron-beam patterned monolayer-protected gold nanoparticle interface films," *Lab Chip*, vol. 10, no. 22, pp. 3058–3060, 2010.

[17] M. Fang, K. Vetelino, M. Rothery, J. Hines, and G. C. Frye, "Detection of organic chemicals by SAW sensor array," *Sens. Actuators B*, vol. 56, nos. 1–2, pp. 155–157, 1999.

[18] D. Matatagui, J. Martí, M. J. Fernández, J. L. Fontecha, J. Gutiérrez, I. Gràcia, C. Cané, and M. C. Horrillo, "Chemical warfare agents simulants detection with an optimized SAW sensor array," *Sens. Actuators B*, vol. 154, no. 2, pp. 199–205, 2011.

[19] K. Reddy, Y. Guo, J. Liu, W. Lee, M. K. Khaing Oo, and X. Fan, "Rapid, sensitive, and multiplexed on-chip optical sensors for micro-gas chromatography," *Lab Chip*, vol. 12, no. 5, pp. 901–905, 2012.

[20] Y. Sun, J. Liu, D. J. Howard, X. Fan, G. Frye-Mason, S.-J. Ja, and A. K. Thompson, "Rapid tandem-column micro-gas chromatography based on optofluidic ring resonators with multi-point on column detection," *Analyst*, vol. 135, no. 1, pp. 165–171, 2010.

[21] J. C. T. Eijkel, H. Stoeri, and A. Manz, "A dc microplasma on a chip employed as an optical emission detector for gas chromatography," *Anal. Chem.*, vol. 72, no. 11, pp. 2547–2552, 2000.

[22] C. Y. Lee, R. Sharma, A. D. Radadia, R. I. Masel, and M. S. Strano, "On-chip micro gas chromatograph enabled by a noncovalently functionalized single-walled carbon nanotube sensor array," *Angew. Chem. Int. Ed.*, vol. 47, no. 27, pp. 5018–5021, 2008.

[23] M. Li, E. B. Myers, H. X. Tang, S. J. Aldridge, H. C. McCaig, J. J. Whiting, R. J. Simonson, N. S. Lewis, and M. L. Roukes, "Nanoelectromechanical resonator arrays for ultrafast, gas-phase chromatographic chemical analysis," *Nano Lett.*, vol. 10, no. 10, pp. 3899–3903, 2010.

[24] E. T. Zellers, M. Morishita, and Q.-Y. Cai, "Evaluating porous-layer open-tubular capillaries as vapor preconcentrators in a microanalytical system," *Sens. Actuators B*, vol. 67, no. 3, pp. 244–253, 2000.

[25] C.-J. Lu, J. Whiting, R. D. Sacks, and E. T. Zellers, "Portable gas chromatograph with tunable retention and sensor array detection for determination of complex vapor mixtures," *Anal. Chem.*, vol. 75, no. 6, pp. 1400–1409, 2003.

[26] C.-J. Lu, W. H. Steinecker, W.-C. Tian, M. C. Oborny, J. M. Nichols, M. Agah, J. A. Potkay, H. K. L. Chan, J. Driscoll, R. D. Sacks, K. D. Wise, S. W. Pang, and E. T. Zellers, "First-generation hybrid MEMS gas chromatograph," *Lab Chip*, vol. 5, no. 10, pp. 1123–1131, 2005.

[27] J. Liu, M. K. Khaing Oo, K. Reddy, Y. B. Gianchandani, J. C. Schultz, H. M. Appel, and X. Fan, "Adaptive two-dimensional microgas chromatography," *Anal. Chem.*, vol. 84, no. 9, pp. 4214 - 4220, 2012.

[28] B. C. Kaanta, H. Chen, G. Lambertus, W. H. Steinecker, O. Zhdaneev, and X. Zhang, "Sensitivity micro-thermal conductivity detector for gas chromatography," presented at the 22nd IEEE Int. Conf. Micro Electro Mech. Syst., Sorrento, Italy, 2009.

[29] B. C. Kaanta, H. Chen, and X. Zhang, "A monolithically fabricated gas chromatography separation column with an integrated high sensitivity thermal conductivity detector," *J. Micromech. Microeng.*, vol. 20, no. 5, p. 055016, 2010.

[30] S. Narayanan, B. Alfeeli, and M. Agah, "Two-port static coated micro gas chromatography column with an embedded thermal conductivity detector," *IEEE Sens. J.*, vol. 12, no. 6, pp. 1893–1900, Jun. 2012.

[31] S. Narayanan and M. Agah, "A micro gas chromatography column with an embedded out-of-plane thermal conductivity detector," in *Proc. Hilton Head*, Hilton Head, SC, 2012, pp. 221–224.

[32] S. I. Shopova, I. M. White, Y. Sun, H. Zhu, X. Fan, G. Frye-Mason, A. Thompson, and S.-J. Ja, "On-column micro gas chromatography detection with capillary-based optical ring resonators," *Anal. Chem.*, vol. 80, no. 6, pp. 2232–2238, 2008.

[33] Y. Sun, J. Liu, G. Frye-Mason, S.-J. Ja, A. K. Thompson, and X. Fan, "Optofluidic ring resonator sensors for rapid DNT vapor detection," *Analyst*, vol. 134, no. 7, pp. 1386–1391, 2009.

[34] Y. Sun and X. Fan, "Optical ring resonators for biochemical and chemical sensing," *Anal. Bioanal. Chem.*, vol. 399, no. 1, pp. 205–211, 2011.

[35] J. Liu, Y. Sun, and X. Fan, "Highly versatile fiber-based optical Fabry-Pérot gas sensor," *Opt. Express*, vol. 17, no. 4, pp. 2731–2738, 2009.

[36] J. Liu, Y. Sun, D. J. Howard, G. Frye-Mason, A. K. Thompson, S.-J. Ja, S.-K. Wang, M. Bai, H. Taub, M. Almasri, and X. Fan, "Fabry-Perot cavity sensors for multipoint on-column micro gas chromatography detection," *Anal. Chem.*, vol. 82, no. 11, pp. 4370–4375, 2010.

[37] J. Liu, N. K. Gupta, K. D. Wise, Y. B. Gianchandani, and X. Fan, "Demonstration of motionless Knudsen pump based micro-gas chromatography featuring micro-fabricated columns and on-column detectors," *Lab Chip*, vol. 11, no. 7, pp. 3487–3492, 2011.

[38] K. Reddy, Y. Guo, J. Liu, W. Lee, M. K. Khaing Oo, and X. Fan, "On-chip Fabry-Pérot interferometric sensors for micro-gas chromatography detection," *Sens. Actuators B*, vol. 159, no. 1, pp. 60–65, 2011.

[39] S. Reidy, G. Lambertus, J. Reece, and R. Sacks, "High-performance, static-coated silicon microfabricated columns for gas chromatography," *Anal. Chem.*, vol. 78, no. 8, pp. 2623–2630, 2006.

[40] K. Reddy and X. Fan, "Self-referenced composite Fabry-Pérot cavity vapor sensors," *Opt. Express*, vol. 20, no. 2, pp. 966–971, 2012.

[41] C. C. Lee, C. Y. Wang, and G. Matijasevic, "Au-In bonding below the eutectic temperature," *IEEE Trans. Compon. Hybr.*, vol. 16, no. 3, pp. 311–316, May 1993.

[42] B. Alfeeli and M. Agah, "Toward handheld diagnostics of cancer biomarkers in breath: Micro preconcentration of trace levels of volatiles in human breath," *IEEE Sens. J.*, vol. 11, no. 11, pp. 2756–2762, Jun. 2011.

[43] J. H. Seo, J. Liu, X. Fan, and K. Kurabayashi, "Effect of thermal desorption kinetics on vapor injection peak irregularities by a microscale gas chromatography preconcentrator," *Anal. Chem.*, vol. 84, no. 15, pp. 6336–6340, 2012.

[44] G. Serrano, D. Paul, S.-J. Kim, K. Kurabayashi, and E. T. Zellers, "Comprehensive two-dimensional gas chromatographic separations with a microfabricated thermal modulator," *Anal. Chem.*, vol. 84, no. 16, pp. 6973–6980, 2012.

Authors' photographs and biographies unavailable at the time of publication.